Composites Research

Vol. 39, No. 1, 21-26 (2026)
DOI: http://dx.doi.org/10.7234/composres.2026.39.1.021
ISSN 2288-2103(Print), ISSN 2288-2111(Online)

Paper

High-Performance Electromagnetic Interference Shielding of Acid-Doped Single-Walled Carbon Nanotubes

Flandy*,, Yongho Joo*,**†**

ABSTRACT: The increasing demand for lightweight electromagnetic interference (EMI) shielding materials has made single-walled carbon nanotubes (SWCNTs) attractive candidates due to their intrinsically high electrical conductivity. In this study, we investigate the effect of acid doping on the EMI shielding (EMI SH) performance of SWCNT films. The films were fabricated via a simple vacuum filtration process and doped using camphor sulfonic acid (CaSA) and chlorosulfonic acid (CSA). A systematic investigation of CaSA concentration revealed only minimal changes in the overall EMI shielding effectiveness. In contrast, increasing the maceration time during CSA post-treatment resulted in a modest enhancement in shielding effectiveness (≈2–3 dB). However, prolonged maceration led to noticeable structural degradation of the SWCNT films. These results indicate that acid doping primarily influences the shielding behavior rather than significantly improving the total shielding effectiveness, highlighting the importance of optimizing acid strength and processing conditions for SWCNT-based EMI shielding materials.

Key Words: Single-walled carbon nanotube, EMI shielding, Camphor sulfonic acid, Chlorosulfonic acid

1. INTRODUCTION

In recent decades, the rapid proliferation of electronic and wireless devices, such as smartphones and laptops, has significantly reshaped modern lifestyles. However, this technological advancement has also introduced unintended challenges, particularly electromagnetic (EM) radiation emitted from electronic devices [1,2]. Excessive EM radiation can disrupt signal transmission and cause malfunction or reduced accuracy of electronic equipment, ultimately affecting device reliability and operational lifetime [3].

Traditionally, high-conductivity metallic materials, such as silver or copper meshes, have been employed to mitigate EMI through reflection or absorption mechanisms [4]. Nevertheless, with the continued advancement of electronic technologies, there is an increasing demand for lightweight, flexible, and highly efficient EMI shielding materials. This demand has driven growing interest in alternative conductive materials, including carbon nanotubes (CNTs), which offer high electrical conductivity, low density, and structural versatility [5,6].

SWCNTs are considered promising materials due to their exceptional electrical and mechanical properties. Molecular-level studies have reported that SWCNTs can exhibit electrical conductivities as high as ~4×10^7 S m^{-1} and tensile strengths exceeding 100 GPa [6-8]. These outstanding properties originate from the unique one-dimensional tubular structure of SWCNTs, which gives rise to either metallic (m-SWCNT) or semiconducting (s-SWCNT) behavior depending on their chirality [4,9-11]. Although the experimentally measured electrical and mechanical properties of macroscopic SWCNT assemblies have not yet reached their intrinsic molecular-level limits, the superior performance observed in existing studies nonetheless highlights SWCNTs as desirable candidates for next-generation EMI shielding materials [12].

To enhance the EMI shielding performance of SWCNTs, various dopants have been introduced to increase electrical conductivity, impart magnetic loss, or improve SWCNT dispersion and network formation. For example, Anilkumar et al.

Received 18 January 2026, received in revised form 2 February 2026, accepted 6 February 2026

*Functional Composite Materials Research Center, Korea Institute of Science and Technology, Jeonbuk 55324, Republic of Korea
**Nanoscience and Technology, KIST School, Korea National University of Science and Technology (UST), Daejeon 34113, Republic of Korea
†Corresponding author (E-mail: yjoo0727@kist.re.kr)

[13] reported the incorporation of polyaniline (PANI), a conductive polymer, to enhance the electrical conductivity of SWCNT composites. Furthermore, CaSA was employed as a secondary dopant to increase conductivity further, resulting in an overall EMI shielding effectiveness of approximately 46 dB in the Ku-band and 28 dB in the X-band. In contrast, Wan et al. [7] demonstrated the use of CSA to densify SWCNT assemblies, significantly improving intertube contacts and achieving an exceptionally high EMI shielding effectiveness of ~101 dB at a thickness of 14.7 μm.

Here, SWCNT films were prepared via a simple vacuum filtration method and subsequently doped with acids to further enhance their EMI shielding performance. Two distinct doping strategies were employed depending on the acid strength: in-situ doping and post-treatment. Moreover, we study the effect of concentration and time on the EMI shielding effectiveness. The result demonstrates how the acid could affect the SWCNT in terms of EMI shielding.

2. EXPERIMENTAL SECTION

2.1 Material

A single-walled carbon nanotube was purchased from Tuball. Sodium dodecyl sulfate (SDS) was purchased from TCl, Camphor sulfonic acid was provided by Alfa Aesar, and chlorosulfonic acid was purchased from Sigma. All reagents were applied exactly as they were given. For all filtration processes, a mixed cellulose ester membrane filter (pore size 0.45 μm, diameter 47 mm) and a PTFE filter membrane (pore size 0.2 μm, diameter 47 mm) were purchased from Advantec, Japan, and a 250 mL glass funnel, a clamp, and a fritted glass support.

2.2 Method

A pristine SWCNT dispersion was prepared by dispersing SWCNT powder in deionized (DI) water containing 2 wt% SDS as a surfactant. The dispersion process consisted of bath sonication for 30 min followed by probe (tip) sonication for 2 h. The resulting dispersion was then centrifuged at 4000 rpm for 40 min to remove agglomerates, and the supernatant was collected for subsequent processing. Two distinct doping strategies were employed depending on the acid strength: (i) in-situ doping, in which 10 mg/mL CaSA was directly added to the SWCNT dispersion. The mixture was sonicated for 30 min to ensure homogeneity, allowed to rest for 2–3 h, and then vacuum-filtered through a cellulose acetate membrane to form SWCNT thin films; and (ii) post-treatment doping, in which pristine SWCNT films were first prepared by vacuum filtration of the dispersion using a polytetrafluoroethylene (PTFE) membrane. The as-prepared films were subsequently immersed in a pure CSA solution for a controlled duration, followed by thorough washing with acetone to remove residual acid. All prepared SWCNT films were evaluated for EMI shielding performance using a WR-90 rectangular waveguide connected to a vector network analyzer (VNA) (Agilent Keysight 8720C). Measurements were conducted with a sample size of 30 mm × 30 mm in the X-band frequency range of 8.19–12.41 GHz. Sample thickness is measured using a surface profiler (Surfcorder ET200, Kosaka Laboratory, Ltd.).

3. RESULT AND DISCUSSION

In this study, SWCNT films were fabricated using a simple vacuum filtration assembly, as illustrated in Fig. 1a. However, SWCNTs inherently tend to form bundles and agglomerates due to strong van der Waals and π–π interactions between

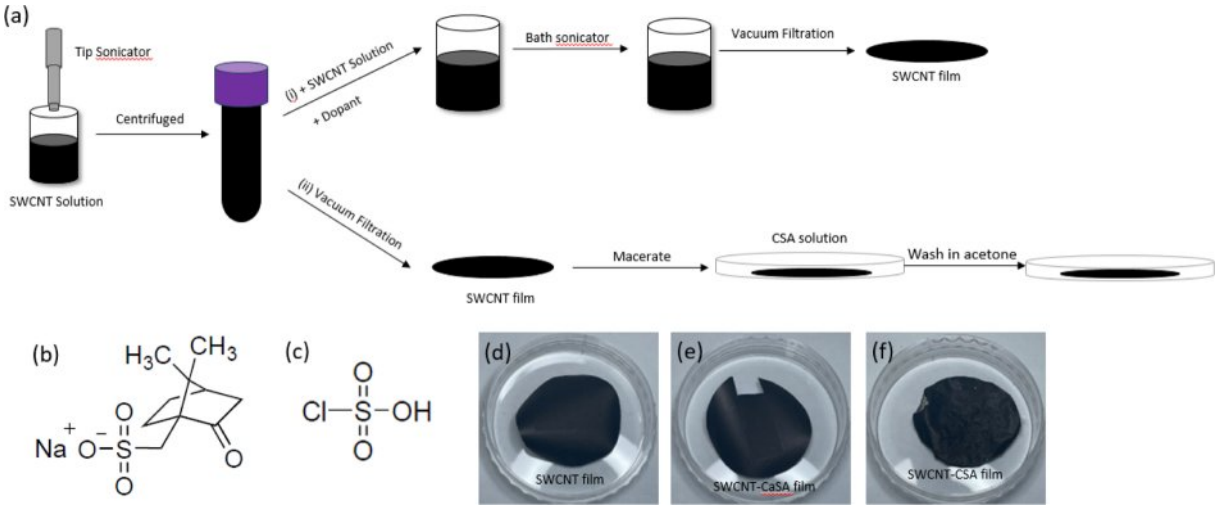

Fig. 1. (a) Schematic illustration of the SWCNT film fabrication and acid-doping processes. Chemical structures of (b) camphor sulfonic acid (CaSA) and (c) chlorosulfonic acid (CSA). Photographs of (d) pristine SWCNT film, (e) CaSA-doped SWCNT film, and (f) CSA-doped SWCNT film

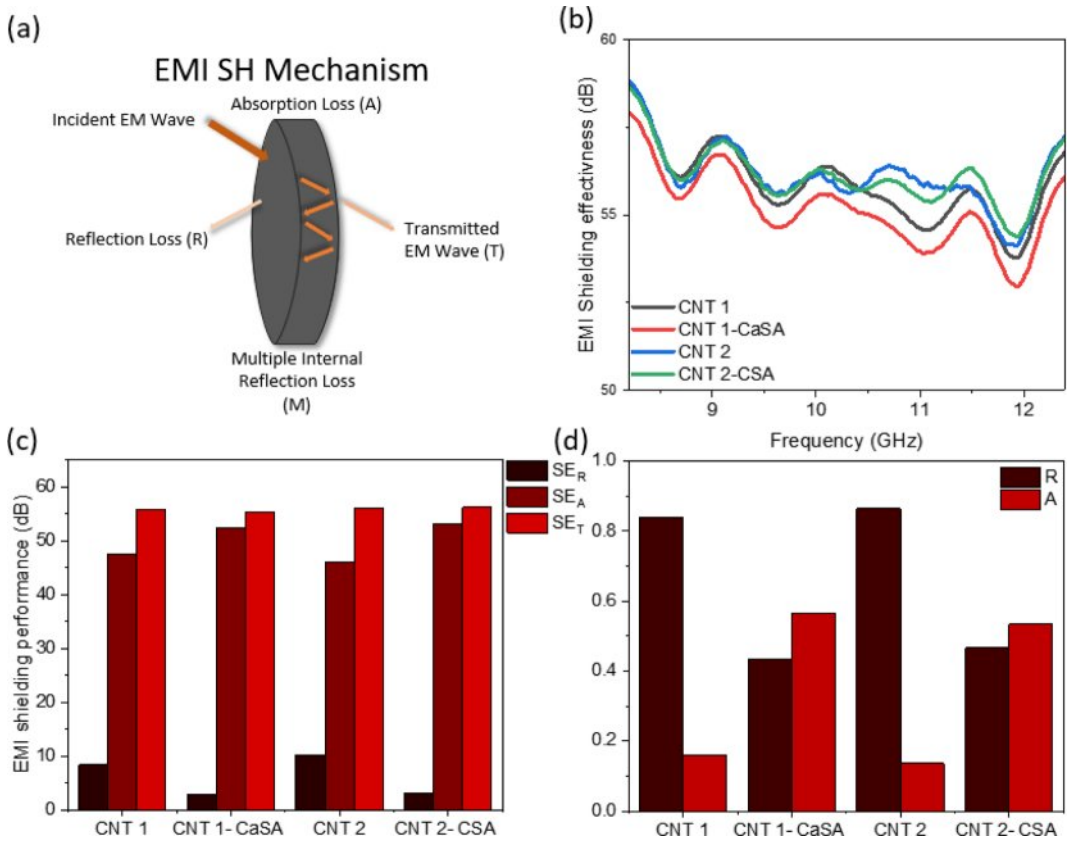

Fig. 2. (a) Schematic illustration of the EMI SH mechanism. (b) EMI shielding effectiveness (SET) of SWCNT, SWCNT-CaSA, and SWCNT-CSA at frequencies ranging from 8.2-12.4 GHz.(c) Comparison of average reflection (SER), absorption (SEA), and total EMI shielding effectiveness (SET). (d) Average R and A coefficient value of SWCNT, SWCNT-CaSA, and SWCNT-CSA

individual nanotubes [11,14]. Therefore, the fabrication process was initiated with the dispersion of SWCNTs in an aqueous medium, assisted by SDS as a surfactant to promote uniform dispersion. Following dispersion, centrifugation was employed to remove impurities and poorly dispersed particles. Agglomerates, and the well-dispersed supernatant was collected for further processing.

Two distinct doping strategies were then applied depending on the acid strength. For the weak acid CaSA, in-situ doping was performed by directly mixing CaSA with the SWCNT dispersion before film formation (Fig. 1b). In contrast, for the strong acid CSA, a post-treatment approach was adopted, in which pristine SWCNT films were first prepared by vacuum filtration and subsequently immersed in CSA to achieve effective doping (Fig. 1c). The resulting doped SWCNT films (Fig. 1d–f) were then evaluated for their EMI shielding performance.

In general, EMI shielding functions by reducing the intensity of incident electromagnetic waves as they propagate through a shielding material. This attenuation occurs primarily through two mechanisms (Fig. 2a): reflection loss (R) and absorption loss (A). The shielding behavior is governed by the electrical and magnetic properties of the material, which enable free or excess charge carriers to oscillate in response to the incident electromagnetic field. Such oscillations result in the reflection of electromagnetic waves at the material surface or their attenuation within the material through absorption, thereby minimizing electromagnetic transmission [15,16].

These shielding mechanisms are experimentally evaluated using a VNA through the measurement of scattering parameters (S-parameters). Based on the measured S-parameters, the EMI shielding effectiveness is calculated in terms of reflection loss (SE_R), absorption loss (SE_A), and total shielding effectiveness (SE_T) using the following equations [17,18]:

$$R = |S_{11}|^2$$

$$T = |S_{21}|^2$$

$$SE_R = -10\log_{10}(1-R)$$

$$SE_A = -10\log_{10}\left(\frac{T}{1-R}\right)$$

$$SE_T = SE_R + SE_A$$

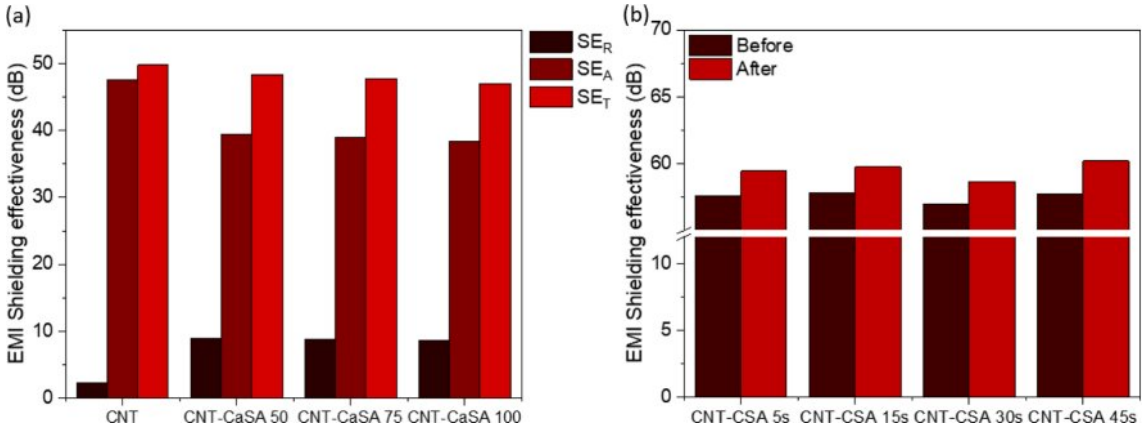

Fig. 3. (a) EMI shielding effectiveness of CNT in different CaSA concentration. (b) EMI shielding effectiveness of CNT in different CSA macerate time

Using the above equations, the EMI shielding effectiveness of pristine and acid-doped SWCNT films was evaluated across the X-band frequency range (Fig. 2b). The results indicate that CaSA and CSA doping lead to only a marginal increase in the SE_T. Specifically, 2 different pristine SWCNT films (CNT-1 and CNT-2) are prepared, with CNT-1 used as the reference sample for CaSA post-treatment and CNT-2 as the reference for CSA post-treatment. However, the SET values remain similar to those of the pristine films even after doping. SET values of approximately 55 dB are obtained for both pristine CNT-1 and CNT-1-CaSA, while both CNT-2 and CNT-2-CSA exhibit SET values of approximately 56 dB (Fig. 2c).

Despite the minimal change in SE_T, a pronounced variation in the R and A coefficients was observed (Fig. 2d). Pristine SWCNT films exhibited reflection-dominated shielding behavior, with R ≈ 0.85 and A ≈ 0.15. In contrast, acid-doped SWCNT films showed a transition toward absorption-dominated shielding, characterized by a reduced R ≈ 0.45 and an increased A ≈ 0.55. This shift indicates a change in the EMI shielding mechanism, from predominantly reflecting incident electromagnetic waves to effectively absorbing a larger fraction of the incident radiation within the material.

Subsequently, the effect of CaSA concentration on the EMI shielding effectiveness was investigated by increasing the CaSA concentration to 50, 75, and 100 mg mL^{-1} (Fig. 3a). The results show that, despite a several-fold increase in CaSA concentration, the total EMI shielding effectiveness remains essentially unchanged across all samples. Meanwhile, extending the maceration duration does not result in a monotonic increase in shielding effectiveness; the comparison between untreated and CSA-treated SWCNT films reveals an overall enhancement of approximately 2–3 dB after CSA maceration(Fig. 3b). However, the use of a strong acid such as CSA presents inherent challenges due to its high reactivity. CSA readily reacts with ambient moisture to generate HCl and H_2SO_4, and prolonged maceration times were observed to induce structural damage to the SWCNT films. These results indicate that while CSA post-treatment can modestly enhance EMI shielding, careful optimization of the maceration duration is required to balance performance improvement and structural integrity.

To investigate chemical modifications induced by acid dop-

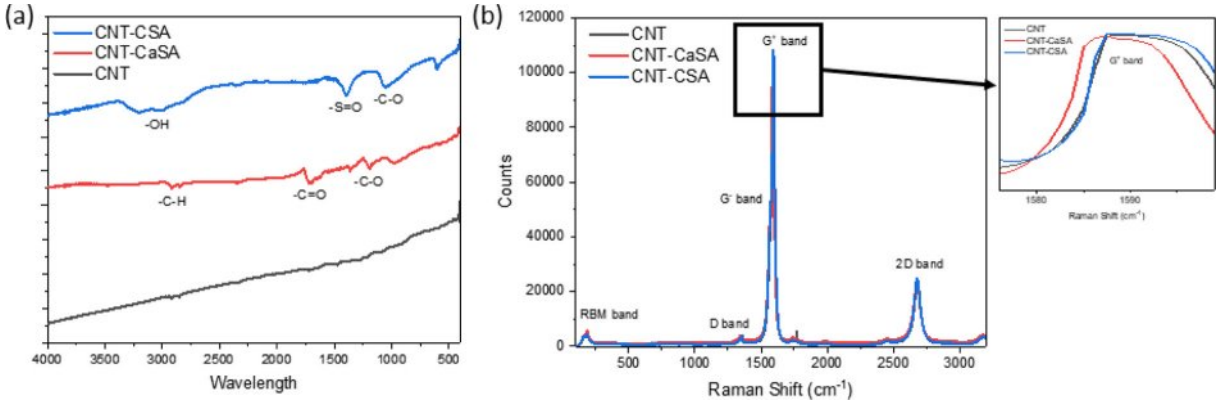

Fig. 4. (a) FTIR results of pristine SWCNT and doped SWCNT, (b)Raman spectroscopy results of pristine SWCNT and doped SWCNT

ing in SWCNT films, FTIR and Raman spectroscopy were employed to assess changes in the physicochemical properties of the carbon surface. The FTIR results indicate that acid doping leads to functionalization of the SWCNT surface. Specifically, CaSA introduces carbonyl-related functional groups, while CSA introduces sulfonate groups onto the SWCNT framework (Fig. 4a).

Raman spectroscopy further supports these findings by evaluating The defect density was evaluated using the intensity ratio of the D band to the G band (I_D/IG), calculated from the respective peak intensities, yielding ID/IG ratios of 0.027, 0.035, and 0.034 for pristine SWCNT, SWCNT-CaSA, and SWCNT-CSA, respectively. Compared to pristine SWCNTs, the acid-doped samples exhibit a higher I_D/I_G ratio, indicating an increase in defect density after the doping treatment, suggesting partial disruption of the sp^2 carbon network. These Raman features are consistent with chemical functionalization of SWCNTs, in agreement with the FTIR results.

In addition, sheet resistance measurements of CSA-doped SWCNT films show a clear reduction in sheet resistance after doping (Fig. 5), indicating enhanced electrical conductivity

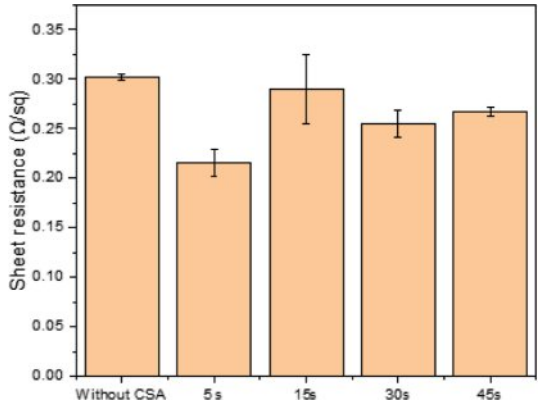

Fig. 5. Sheet resistance result of pristine SWCNT and CSA-doped SWCNT

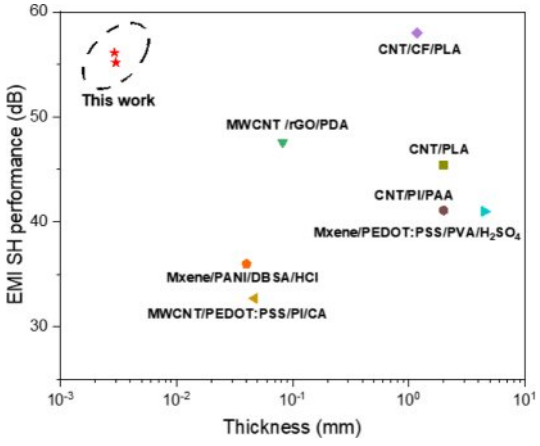

Fig. 6. EMI SH performance of CNT-CaSA and CNT-CSA compared to other similar material

consistent with increased carrier concentration induced by acid doping. Collectively, these chemical and electrical modifications are consistent with reduced reflection and enhanced absorption-dominated EMI shielding behavior.

Next, we compare the EMI SH performance of our work with the reported material that was doped using acid (Fig. 6) [19-25]. Importantly, compared to other material our material exhibits exceptional EMI SH performance with a thinner film

4. CONCLUSIONS

In this work, the effects of camphor sulfonic acid (CaSA) and chlorosulfonic acid (CSA) doping on the EMI shielding performance of SWCNT films were systematically investigated. The results reveal that increasing the CaSA concentration induces only a negligible change in the total EMI shielding effectiveness. Nevertheless, a pronounced transition in the shielding mechanism was observed, with the dominant contribution shifting from reflection-dominated to absorption-dominated behavior. Furthermore, a modest enhancement in EMI shielding effectiveness of approximately 2–3 dB was achieved by increasing the CSA maceration duration. These findings demonstrate that acid doping primarily modulates the EMI shielding mechanism rather than significantly increasing the overall shielding effectiveness, highlighting the importance of dopant selection and processing conditions in tailoring SWCNT-based EMI shielding materials.

ACKNOWLEDGEMENT

This work was supported by the Korea Institute of Science and Technology (KIST, Korea) Institutional Program (YJ). This work was supported by the National Research Foundation of Korea (NRF) grant funded by the Korean government (MSIT) (No. RS-2023-00208313, YJ). This work was supported by the Glocal University 30 Project Fund of Gyeongsang National University in 2024.

REFERENCES

1. Zeng, Z., Wang, G., Wolan, B. F., Wu, N.,Wang, C., Zhao, S., Yue, S., Li, B., He, W., and Liu, J., "Printable aligned single-walled carbon nanotube film with outstanding thermal conductivity and electromagnetic interference shielding performance," *Nano-Micro Letters*, 2022, 14(1), 179.
2. Chen, Y.-J., Dung, N. D., Li, Y.-A., Yip, M.-C., Hsu, W.-K., and Tai, N.-H., "Investigation of the electric conductivity and the electromagnetic interference shielding efficiency of SWCNTs/GNS/PAni nanocomposites," *Diamond and Related Materials*, 2011, 20(8), 1183-1187.
3. Kumaran, R., Kumar, S. D., Balasubramanian, N., Alagar, M., Subramanian, V., and Dinakaran, K., "Enhanced electromagnetic interference shielding in a Au–MWCNT composite nanostructure dispersed PVDF thin films," *The Journal of Physical*

Chemistry C, 2016, 120(25), 13771-13778.
4. Yu, I., Ko, J., Kim, T.-W., Lee, D. S., Kim, N. D., Bae, S., Lee, S.-K., Choi, J., Lee, S. S., and Joo, Y., "Effect of sorted, homogeneous electronic grade single-walled carbon nanotube on the electromagnetic shielding effectiveness," *Carbon*, 2020, 167, 523-529.
5. Nguyen, T. T. L., Cho, S. J., Ko, J., Nguyen, D. C. T., Kim, M. W., Kim, N. D., Lee, D. S., and Joo, Y., "Exceptional electromagnetic interference shielding using single-walled carbon nanotube/conductive polymer composites films with ultrathin, lightweight properties," *Carbon*, 2024, 230, 119567.
6. Ji, Y., Jang, J. M., Kim, J. Y., Choi, E., Jeong, H., Lee, C. H., Lee, S., Kwak, Y., Cho, Y., and Lee, H., "SWCNT/MWCNT binderless hybrid hydrogel: Towards large-scale high-performance EMI shielding coating at commercial level," *Carbon*, 2025, 238, 120250
7. Wan, Y.-J., Wang, X.-Y., Li, X.-M., Liao, S.-Y., Lin, Z.-Q., Hu, Y.-G., Zhao, T., Zeng, X.-L., Li, C.-H., and Yu, S.-H., "Ultrathin densified carbon nanotube film with "metal-like" conductivity, superior mechanical strength, and ultrahigh electromagnetic interference shielding effectiveness. *ACS nano*, 2020, 14(10), 14134-14145.
8. Kharlamova, M. V., and Kramberger, C., "Applications of filled single-walled carbon nanotubes: Progress, challenges, and perspectives," *Nanomaterials*, 2021, 11(11), 2863.
9. Arnold, M. S., Green, A. A., Hulvat, J. F., Stupp, S. I., and Hersam, M. C., "Sorting carbon nanotubes by electronic structure using density differentiation," *Nature nanotechnology*, 2006, 1(1), 60-65.
10. Huang, Y., Li, N., Ma, Y., Du, F., Li, F., He, X., Lin, X., Gao, H., and Chen, Y., "The influence of single-walled carbon nanotube structure on the electromagnetic interference shielding efficiency of its epoxy composites," *Carbon*, 2007, 45(8), 1614-1621.
11. Vijayaraghavan, D., "Aggregates of single-walled carbon nanotube bundles in a surfactant solution," *Journal of Molecular Liquids*, 2015, 209, 440-446.
12. Gong, X., Hu, T., Zhang, Y., Zeng, Y., Zhang, Y., Jiang, Z., Tan, Y., Zou, Y., Wang, J., and Dai, J., "Trunk-inspired SWCNT-based wrinkled films for highly-stretchable electromagnetic interference shielding and wearable thermotherapy," *Nano-Micro Letters*, 2024, 16(1), 243.
13. Anilkumar, R., Abhilash, A., Indhu, K., Sunil, M., Das Krishna, D., John, H., and Aanandan, C., "CSA-doped PANI-CNT nano composites for Ku band microwave shielding applications," *Fullerenes, Nanotubes and Carbon Nanostructures*, 2024, 32(12), 1193-1201.
14. Dai, J., Fernandes, R. M., Regev, O., Marques, E. F., and Furo, I., "Dispersing carbon nanotubes in water with amphiphiles: dispersant adsorption, kinetics, and bundle size distribution as defining factors," *The Journal of Physical Chemistry C*, 2018, 122(42), 24386-24393.
15. Kondawar, S. B., and Modak, P. R., "Theory of EMI shielding," In Materials for Potential EMI Shielding Applications, Elsevier, 2020, pp 9-25.
16. Chung, D., "Materials for electromagnetic interference shielding," *Materials Chemistry and Physics* 2020, 255, 123587.
17. Isari, A. A., Ghaffarkhah, A., Hashemi, S. A., Wuttke, S., and Arjmand, M., "Structural design for EMI shielding: from underlying mechanisms to common pitfalls," *Advanced Materials*, 2024, 36(24), 2310683.
18. Wang, H., Li, S., Liu, M., Li, J., and Zhou, X., "Review on shielding mechanism and structural design of electromagnetic interference shielding composites," *Macromolecular Materials and Engineering*, 2021, 306(6), 2100032.
19. Sharma, S., Lee, J., Dang, T. T., Hur, S. H., Choi, W. M., and Chung, J. S., "Ultrathin freestanding PDA-Doped rGO/MWCNT composite paper for electromagnetic interference shielding applications," *Chemical Engineering Journal*, 2022, 430, 132808.
20. Xie, H.-H., Lu, Y., Zhao, X.-L., Zeng, J.-B., Wang, M., and Li, Y.-D., "Ultrahigh strength poly(lactic acid) composites with superior EMI shielding performance enabled by synergistic effect of short carbon fibers and carbon nanotubes," *Composites Science and Technology*, 2025, 261, 111045.
21. Liu, X.-C., Tian, L.-Y., Bao, Z.-L., Zhang, Y.-S., Qian, P.-F., Geng, W.-H., Zhang, D., Zhu, Q., and Geng, H.-Z., "Caffeic-acid-functionalized MWCNTs and PEDOT: PSS formed composite flexible films with "reinforced concrete" structure for electrical heating and EMI shielding," *ACS Applied Materials & Interfaces*, 2024, 16(17), 22391-22402.
22. Li, P., Wang, H., Ju, Z., Jin, Z., Ma, J., Yang, L., Zhao, X., Xu, H., and Liu, Y., "$Ti_3C_2T_x$ MXene-and sulfuric acid-treated double-network hydrogel with ultralow conductive filler content for stretchable electromagnetic interference shielding," *ACS nano*, 2024, 18(4), 2906-2916.
23. Wang, Y.-Y., Zhou, Z.-H., Zhou, C.-G., Sun, W.-J., Gao, J.-F., Dai, K., Yan, D.-X., and Li, Z.-M., "Lightweight and robust carbon nanotube/polyimide foam for efficient and heat-resistant electromagnetic interference shielding and microwave absorption," *ACS Applied Materials & Interfaces*, 2020, 12(7), 8704-8712.
24. Xu, Z., Dou, T., Wang, Y., Zuo, H., Chen, X., Zhang, M., and Zou, L., "Three-dimensional-printed carbon nanotube/polylactic acid composite for efficient electromagnetic interference shielding," *Polymers*, 2023, 15(14), 3080.
25. Zhang, Y., Wang, L., Zhang, J., Song, P., Xiao, Z., Liang, C., Qiu, H., Kong, J., and Gu, J., "Fabrication and investigation on the ultra-thin and flexible $Ti_3C_2T_x$/co-doped polyaniline electromagnetic interference shielding composite films," *Composites Science and Technology*, 2019, 183, 107833.